A Source Identification Problem for the Electrical Activity of Brain During Hand Movement

A source identification problem for the electrical activity of brain during hand movement

P. Di Barba[*], F. Freschi[**], M. E. Mognaschi[*], A. Pichiecchio[***], M. Repetto[**], A. Savini[*], A. Vultaggio[***]

[*] Department of Electrical Engineering, University of Pavia
Via Ferrata 1, 27100 Pavia, Italy

[**] Department of Electrical Engineering, Politecnico di Torino,
Corso Duca degli Abruzzi 24,
10129 Torino, Italy

[***] I.R.C.C.S. Neurological Institute "C. Mondino",
Via Mondino 2, 27100 Pavia, Italy

Abstract— A field source reconstruction of the dipoles modeling the activated area of the brain, while a subject performs the task of the voluntary motion of the hand, is solved. Experimental data resulting from fMRI are used for constraining the position of the equivalent dipole.

I. Introduction

Magnetic Resonance Imaging (MRI) and functional Magnetic Resonance Imaging (fMRI) techniques have good spatial resolution, but poor time resolution, because the time required to scan the head is longer than the characteristic time of brain activation. Electroencephalographic (EEG) technique, on the contrary, has a good time resolution, but poor spatial resolution. A good idea is to couple these two techniques in order to identify, using a field model, the brain areas activated during a simple task performed by a person [1]. In particular, fMRI technique is useful for determining a priori the position of the source or constraining the source position; EEG technique gives information about the temporal evolution of the source. For this research fMRI and EEG data have been recorded, but only fMRI information is used for source reconstruction because the problem is supposed to be static.

II. Experiments

For the sake of building the 3D model of the head, MR images have been acquired using a Philips Intera 1.5 Tesla Gyroscan scanner. A high resolution T1-weighted anatomical image was acquired in a sagittal orientation using a Fast Field Echo (FFE) sequence covering the whole brain with 160 slices.

In order to identify the brain area activated during the task, a fMRI study was performed. Functional data were acquired using a T2*-weighted echo-planar imaging sequences with a repetition time equal to 3 s.

The task to be studied is a motor stimulus consisting of a repetitive flexion-extension of the five digits of the right hand carried out by the volunteer with a block design, where five period of activation were alternated with five period of rest.

Statistical analysis was performed using SPM5 (http://www.fil.ion.ucl.ac.uk/spm). Images were realigned to the first one to correct for subject motion, spatially normalized according to the MNI stereotactic space and smoothed with a 6 mm 3D Gaussian filter.

Changes in Blood Oxygenation Level Dependent (BOLD) signal associated with the performance of the motor task were based on the application of the general linear model [2] voxel-by-voxel. Significant contrast was assessed using t statistical parametric maps (SPMt). The activations were recorded below a threshold of $P<0.05$ corrected for multiple comparisons.

Activations were projected into the normalized anatomical image.

Greater activation was found in the primary motor cortex (Brodmann areas (BA) 3,4), the primary sensorimotor cortex (BA 6), in the anterior prefrontal (BA 10) and in the middle temporal gyrus (BA 41-42). The prefrontal area is involved in memory retrieval and executive function and it is probably active because of the attention paid by the volunteer in performing the task. The temporal area is involved in hearing processes; this is due to the noise inside the MR chamber. Among the three, the area related to the hand was taken into account for the identification problem in this paper. This area, belonging to the primary motor cortex and to the somatosensory cortex, is about 20 mm × 20 mm × 20 mm and is shown in Fig. 1.

Fig. 1 – fMRI images: the area related to hand movement is highlighted; bottom-right: experimental setup for EEG.

In order to assess the magnitude of scalp potential, EEG technique was applied to the same volunteer performing the task, outside the MRI chamber (see Fig. 1, bottom-right). Nineteen electrodes were positioned on the scalp using the 10-20 system, one more electrode was put on the opponens pollicis muscle to record the electromyographic signal. The EEG signals were filtered with a band-pass filter in the range [0.5;1000] Hz. Because of the noise affecting signals, the registrations were repeated 200 times and the average is considered. This way one has the so called event-related potentials.

The signals so recorded have a magnitude of μV. Analyzing the 2D potential map in the range of time [-200 ms,+200 ms] with respect to the appearance of movement of the hand (initial point of the electromyographic signal) it is possible to note that two main areas are activated. One area is

related to the motor cortex, controlater to the hand moved, and the other is a frontal area, as shown in Fig. 2a and Fig. 2b, respectively.

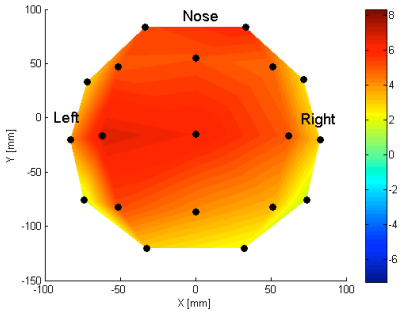

Fig. 2a – Evoked-related potential map about 100 ms before the appearance of hand movement; the potential scale is in μV.

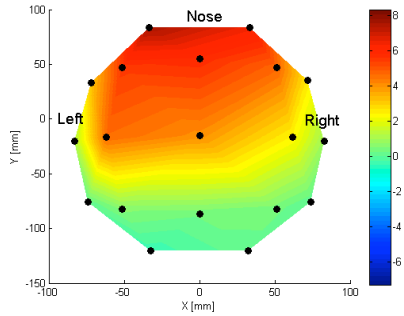

Fig. 2b – Evoked-related potential map about 20 ms after the appearance of hand movement; the potential scale is in μV.

These results about the two areas, which are valid for the whole temporal range considered, are in agreement with the fMRI results. The third area (the temporal one) shown in fMRI does not seem to be active in these registration. This could be explained by the fact that the potential registrations were made outside the MRI chamber in a noiseless environment.

III. Field Analysis

A three-dimensional model of the head of the person subject to experiments was built, as shown in Fig. 3.

The head anatomy was reconstructed using semi-automatic procedures, starting from the images provided by MRI. The voxels of the model have dimension 1.14 mm × 1.14 mm × 1.5 mm: 1.6 10^6 nodes belong to the whole model.

Seven different tissues are considered, namely grey matter, white matter, cerebrospinal fluid, muscle, bone, fat, skin. The electrical conductivity of these tissues is shown in Table I.

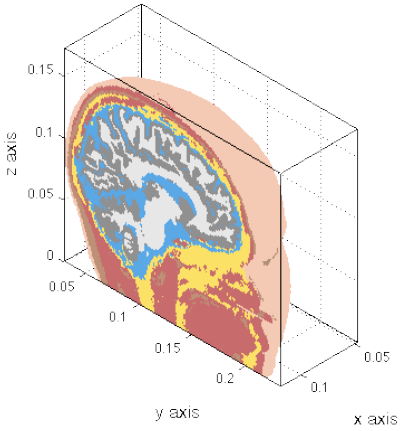

Fig. 3 – 3D model of the head of the person under study (after MRI)

TABLE I
CONDUCTIVITY OF BIOLOGICAL TISSUES AT LOW FREQUENCIES

Tissue	Conductivity [Sm^{-1}]
Grey matter	0.33
White matter	0.14
Cerebrospinal fluid	1.54
Muscle	0.1
Bone	0.00625
Fat	0.04
Skin	0.43

The sources of the conduction field are current dipoles representing the activated areas in the brain. Due to the slow variation of electric sources in the brain, the electric potential φ, to be recorded on the scalp, is governed by the electrostatic approximation of Maxwell's equation:

$$\nabla \cdot (\sigma \nabla \varphi) = \nabla \cdot \vec{J}_S \qquad (1)$$

where σ is the electrical conductivity, and $\vec{J}_S$ is the dipole current density, which in general is a time-varying function.
Neumann condition is applied to all surface nodes, while the reference potential is set on the left earlobe.
For solving problem (1) the cell method is used. The cell method implements an algebraic formulation of the field problem and associates potential to mesh nodes and current to mesh edges [3]. Problem (1) reads

$$\tilde{D} M_\sigma G \varphi = \tilde{D} i_s \qquad (2)$$

with $\tilde{D}$ the dual discrete divergence operator (volume-face incidence matrix equal to G^T), M_σ the conductance constitutive matrix, G the discrete gradient operator (edge-node incidence matrix) and i_s the edge current. The solution to problem (2) is

$$\varphi = K^{-1} \tilde{D} i_s \qquad (3)$$

with $K = \tilde{D}M_\sigma G$, stiffness matrix, factorized in a suitable way.

Because in this problem the point of interest for potential calculation is only the position of the EEG electrodes, it is convenient to restrict the calculation to the subset of those surface electrodes. This can be done by means of a projection matrix P

$$\hat{\varphi} = P\varphi \tag{4}$$

The a priori knowledge on the position of the sources coming from fMRI results can be taken into account by means of an interpolation matrix Q such that

$$i_s = Qi \tag{5}$$

The problem now reads:

$$\hat{\varphi} = PK^{-1}G^T Q\ i = L\ i \tag{6}$$

The L matrix is the so-called lead field matrix, which maps the source vector to scalp potential in selected points. The advantage of using this matrix for solving the problem is the reduction in computational cost.

IV. Inverse Problem

The inverse problem reads as follows: knowing the head anatomy of the person subject to MRI, the electromagnetic properties of the biological tissues, the position of the activated area (from fMRI) and the electrical activity on the scalp, identify the orientation and the magnitude of the equivalent dipole which models the area activated during the task.

The electrical activity on the scalp is calculated numerically a priori and it is hereinafter called benchmark solution. Two different cases for benchmark solutions have been considered:

1) *one dipole positioned in the center of the activated area*
2) *two dipoles positioned inside the activated area*

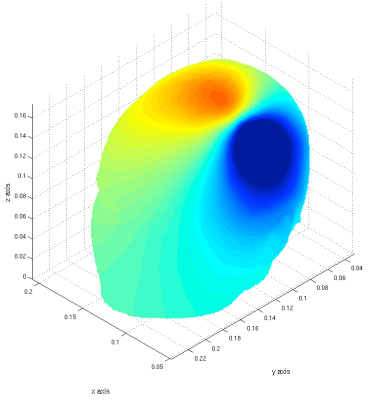

Fig. 4 – Potential map given by one dipole set in the activated area and calculated by means of the cell method.

The activated area is built according to the information given by fMRI and shown in Fig. 1. The benchmark solution (case 1) is shown in Fig. 4

From the computational viewpoint, the solution of the inverse problem is based on the minimization of a suitable functional; to this end two different approaches are used.

The first approach defines the functional to be minimized as the error between computed and benchmark potential in the scalp positions corresponding to the EEG electrodes. Hence, the problem reads: find the set x of variables characterizing the source dipole, which minimizes the error functional

$$\varepsilon(x) = \frac{\left\|\varphi(x) - \hat{\varphi}\right\|_2}{n\left\|\hat{\varphi}\right\|_2} = \frac{1}{n}\sqrt{\frac{\sum_{i=1}^{n}\left[\varphi_i(x) - \hat{\varphi}_i\right]^2}{\sum_{i=1}^{n}\hat{\varphi}_i^2}} \tag{7}$$

where $\hat{\varphi}$ is the benchmark solution, $\varphi(x)$ is the computed solution and n the number of points in which the field is evaluated (n=19, which are the electrode positions).

Because each dipole is characterized by 6 parameters (3 for the position and 3 for the magnitude), but the position is supposed to be known from fMRI, in case 1 only 3 variables have to be identified; in case 2 the variables to be identified are 6, i.e. 3 for each dipole.

The error minimization is driven by a stochastic algorithm, because this kind of problem is known to have many local minima. In particular, a 1+1 evolution strategy called ESTRA (from one parent an offspring is generated and the fittest individual between parent and offspring is selected) is used. ESTRA was successfully used in [4], where the reconstruction of a single dipole source was solved considering an analytical model of the head.

The unknowns of the second approach are current values i_k (continuous) and binary values δ_k for each edge k. Variable δ_k defines the on/off status of the k-th edge current i_k. In the actual example the number of possible active edges is about 3000, which are the edges of the region identified by means of fMRI analysis.

The algorithm should minimize the number of sources of a specified potential map [5], generalized here for arbitrary oriented dipoles. This can be formulated as a linear combination of the binary variables:

$$\min \sum_k \delta_k \tag{8}$$

This is a Mixed Integer Linear Programming (MILP) problem, subject to the following constraints.

A first set of inequality constraints is the relation between continuous and binary variables in each edge:

$$-I_{max}\delta_k \le i_k \le I_{max}\delta_k \tag{9}$$

The reconstruction of electrode potentials can be imposed as an equality constraint:

$$Li = \hat{\varphi} \tag{10}$$

It is useful to relax this constraint, since recorded scalp potential are affected by measurement uncertainties. To be less prone to noise on scalp potentials, (10) is reformulated as an inequality constraint:

$$(1-\alpha)\hat{\varphi} \le \mathrm{Li} \le (1+\alpha)\hat{\varphi} \qquad (11)$$

where $\alpha > 0$ is an estimation of measurement uncertainties. When $\hat{\varphi} < 0$ the inequality sign of (11) must be reversed.

In this work for solving problem (8) a commercial code that implements branch-and-cut technique [6] is adopted.

Hence, in ESTRA approach the fMRI results are used to localize the source of the problem and magnitude and orientation have to be identified, while in MILP approach fMRI results are used to constrain the solution, i.e. they give boundaries for the variables to be identified.

V. Results

All the optimization problems are solved considering different situations: no noise, white noise of 5%, 10% and 15% in magnitude with respect to signal.

The starting point is x_0=[0.5 0.5 0.5] for case 1 and x_0=[0.5 0.5 0.5 0.5 0.5 0.5] for case 2. The variation range for each variable is [-1;1] Am. The results obtained applying ESTRA to case 1 and case 2 are shown in Table II and Table III, respectively. To better show the goodness of the solution, a relative error $\varepsilon_x(x)$ on the reconstructed solution is introduced:

$$\varepsilon_x(x) = \frac{\left\| x - \hat{x} \right\|_2}{m \left\| \hat{x} \right\|_2} \qquad (12)$$

where $\hat{x}$ is the set of parameters of the benchmark solution dipole and $m = \dim(\hat{x})$.

TABLE II
RESULTS OBTAINED WITH ESTRA – CASE 1

	ε(x)	$\varepsilon_x(x)$	Iterations
No noise	$4.393\ 10^{-6}$	$2.93\ 10^{-5}$	461
Noise 5%	$1.13\ 10^{-3}$	$9.66\ 10^{-3}$	611
Noise 10%	$2.04\ 10^{-3}$	$8.96\ 10^{-3}$	611
Noise 15%	$3.28\ 10^{-3}$	$3.31\ 10^{-2}$	415

TABLE III
RESULTS OBTAINED WITH ESTRA – CASE 2

	ε(x)	$\varepsilon_x(x)$	Iterations
No noise	$8.896\ 10^{-4}$	$6.7\ 10^{-2}$	20981
Noise 5%	$8.616\ 10^{-4}$	$3.2\ 10^{-2}$	7357
Noise 10%	$1.519\ 10^{-3}$	$1.2\ 10^{-1}$	6607
Noise 15%	$1.907\ 10^{-3}$	$1.3\ 10^{-1}$	5643

Many other runs of the optimization problem were made considering different dipole strength and orientation; the order of magnitude of the error functional ε(x) found, confirmed always the results above.

Applying the MILP method for case 1, the number of dipole found was correctly one. In particular the results found by adding noise are shown in Table IV.

TABLE IV
RESULTS OBTAINED WITH MILP – CASE 1

	ε(x)	$\varepsilon_x(x)$	Elapsed time [s]
No noise	$1.64\ 10^{-8}$	$2.29\ 10^{-7}$	87.6
Noise 5%	$8.11\ 10^{-4}$	$4.20\ 10^{-3}$	152.9
Noise 10%	$3.22\ 10^{-3}$	$1.16\ 10^{-1}$	5.5
Noise 15%	$1.38\ 10^{-3}$	$1.05\ 10^{-1}$	3.7

Also for case 2, MILP was able to find two sources and results are shown in Table V.

TABLE V
RESULTS OBTAINED WITH MILP – CASE 2

	ε(x)	$\varepsilon_x(x)$	Elapsed time [s]
No noise	$6.74\ 10^{-6}$	$3.89\ 10^{-5}$	965.0
Noise 5%	$2.43\ \ 10^{-3}$	$9.17\ 10^{-2}$	104.0
Noise 10%	$5.42\ 10^{-3}$	$7.13\ 10^{-2}$	112.0
Noise 15%	$4.12\ 10^{-3}$	$8.12\ 10^{-2}$	31.0

MILP run on a 2 quad-core Intel Xeon E5440, 2.83 GHz – 32 GB RAM, while ESTRA run on a Pentium 4, 3 GHz – 2GB RAM and it takes about 0.15 s for 100 iterations.

The precision gained with MILP is comparable with that obtained with ESTRA. Moreover, MILP method was able to find the right location of the sources in all problems, while in ESTRA the position was set a priori by fMRI.

VI. Conclusion

A preliminary work for the identification of electrical brain activity during hand movement has been presented. Two different numerical techniques using experimental data, mainly from MRI and fMRI, were employed. The performances of the two methods seem to be comparable in terms of precision gained.

In future works the challenge will be solving the problem taking into account the whole time window in which the task is done. For this purpose EEG data will be used together with MRI and fMRI data.

VII. Acknowledgment

The authors are grateful to Mr. Roberto Callieco for the technical help in the experimental part of the work.

VIII. References

[1] P. Ritter, A. Villringer**, "**Simultaneous EEG-fMRI", Neuroscience Biobehavorial Rev, 30(6), pp. 823-38, 2006.

[2] K.J. Friston, A.P. Holmes, J.-B. Poline, P.J. Grasby, S.C.R. Williams, R.S.J. Frackowiak, and R. Turner, " Analysis of fMRI time-series revisited", *NeuroImage* **2:**45–53, 1995a.

[3] F. Freschi, L. Giaccone, and M. Repetto, "Educational value of the algebraic numerical methods in electromagnetism", COMPEL, vol. 27, no. 6, pp. 1343–1357, 2008.

[4] P. Di Barba, M.E. Mognaschi, G. Nolte, R. Palka, A. Savini, "Source identification based on regularization and evolutionary computing in biomagnetic fields", COMPEL, vol. 29, 2010.

[5] F. Freschi, "Brain source localization: a MILP approach", IEEE Trans. Mag., Vol. 46, No. 8, 2010, pp. 3429-3432.

[6] A. Martin, "General mixed integer programming: Computational issues for branch-and-cut algorithms," in Computational Combinatorial Optimization,ser. LNCS. Springer-Verlag, no. 2241, pp. 1–25, 2001.